Robotics and Computer–Integrated Manufacturing 97 (2026) 103108

Contents lists available at ScienceDirect

Robotics and Computer-Integrated Manufacturing

journal homepage: www.elsevier.com/locate/rcim

Full length article

A framework for integrated design of human–robot collaborative assembly workstations

Martina Salami [a], Pietro Bilancia [a,*], Margherita Peruzzini [b], Marcello Pellicciari [a]

[a] Department of Sciences and Methods for Engineering, University of Modena and Reggio Emilia, Reggio Emilia, Italy
[b] Department of Industrial Engineering, University of Bologna, Bologna, Italy

ARTICLE INFO

Keywords:
Collaborative robotics
Collaborative assembly
Integrated design framework
Task allocation
Human–robot simulation
Virtual prototyping

ABSTRACT

Collaborative robotics is increasingly considered in manufacturing to improve efficiency while reducing operators physical and cognitive workloads. However, the lack of comprehensive methodologies has limited the consistent implementation of human–robot collaborative workstations across industries. Existing approaches are often fragmented, require robotics expertise, and pose challenges for non-experts, leading to suboptimal station designs and inefficient task allocation. This study presents a structured design framework to transition traditional assembly processes into collaborative ones. The framework provides a practical, scalable solution for optimizing collaborative workstations, balancing performance, ergonomics, and industrial applicability. It starts from the analysis of the assembly tasks, followed by classification and allocation between human operators and robots, and concludes with virtual prototyping and performance optimization through simulation using a commercial tool. The adopted methodology integrates task analysis, ergonomic assessment, and workspace design to ensure accessible and efficient implementation. Validated through two industrial case studies involving a gear pump and a worm gearbox, the approach demonstrated significant reductions in cycle time and notable improvements in the ergonomic working conditions. Additionally, physical prototyping and testing conducted within a research collaborative cell further confirmed the achieved results.

1. Introduction

In the modern era of Industry 4.0 [1], manufacturing is progressively moving towards small batch production of customized products. This evolution demands the adoption of flexible, reprogrammable automation systems capable of dynamically adapting to diverse production requirements [2]. Despite significant advancements in robotics over the past decades, fully autonomous systems still face challenges in certain processes. These include precision assembly and the handling of delicate objects, complex shapes, or materials with non-standard properties, often requiring human intervention due to built-in limitations [3,4]. In this context, collaborative robots (usually referred to as cobots), have emerged as a promising solution to these challenges. They enable the development of efficient and flexible collaborative workstations that combine the precision and strength of robots with the adaptability and decision-making skills of human operators. In the recently introduced Industry 5.0 vision [5], the synergy between human and robotic capabilities is further emphasized. This integration aims to enhance overall process efficiency, reducing the physical and cognitive workload on human operators [6], and increasing the adaptability of production lines. Modern cobotics embodies this philosophy, combining the qualities of humans and robots to create a more balanced and high-performing production environment. Nevertheless, despite its potential, the effective implementation of industrial collaborative workstations presents its own challenges.

Research in collaborative robotics has experienced a significant growth in recent years, focusing on critical topics such as human–robot interaction [7,8], object manipulation [9], safety [10,11], programming [12], and ergonomics [13]. However, many of these advancements remain confined to academic laboratories and fail to translate into standardized methods, procedures, and tools suitable at industrial level. This gap between academic progress and industrial practice creates a fragmented and chaotic landscape, hindering the effective adoption of collaborative production systems in real-world settings. Indeed, while many companies are investing in cobot technologies, the implemented workstations often reveal significant shortcomings, such as suboptimal designs or improper task allocations. In numerous instances, cobots are deployed for tasks better suited to industrial robots (e.g. autonomous material feeding on machines or pick-and-place operations in confined areas), resulting in poorly conceived or

* Corresponding author.
E-mail address: pietro.bilancia@unimore.it (P. Bilancia).

https://doi.org/10.1016/j.rcim.2025.103108
Received 11 August 2025; Accepted 11 August 2025
Available online 30 August 2025

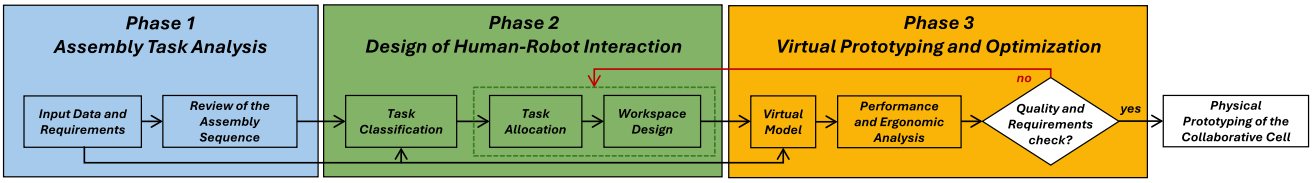

Fig. 1. Overview of the proposed design framework, consisting of three phases, with a visual representation of the blocks within each phase. Input/output flow is shown for each block, along with an iterative loop (highlighted by the red arrow) involving four blocks.

null human–robot interactions. In other cases, cobots are merely used within demo cells, without full integration into real production lines.

The design of collaborative workstations is inherently complex, as it requires the integration of multiple disciplines, while balancing safety, efficiency and flexibility. Assembly operations are one of the most prominent applications for cobot implementation [14,15]. At industrial level [16], these processes range from fully manual operations (performed solely by operators) to semi-automated workflows (alternating stations with humans or machines) and fully automated systems (e.g. autonomous fenced robotic cells), depending on the product characteristics and overall production requirements [17]. In many cases, especially when the human role is essential (i.e. cases demanding real-time decision-making or intricate manipulations) a cobot can be very useful. This is also true for tasks that involve repetitive movements, heavy lifting, or uncomfortable postures. In these situations, using a cobot can boost production efficiency and reduce physical strain and fatigue-related errors.

Despite the potential of cobotics in assembly operations, there remains a notable lack of practical, comprehensive, and accessible solutions and guidelines for effectively designing collaborative cells. As mentioned earlier, many academic research findings do not translate into standardized approaches that are applicable in industrial settings, highlighting the need for robust, efficient, yet simple methods and tools that enable industrial users to effectively implement collaborative systems. Clear guidelines are essential to balance all key factors in the design process, ensuring both productivity and the safety and comfort of human operators. Bridging these gaps will enable the development of systems that foster smoother and more effective human–robot collaboration.

Recent contributions in this direction include the work of Saenz et al. [18], who focused on workstation design with a safety-oriented approach, emphasizing the challenges and the non-linearity of the decision-making process that must be followed. Although the process flow for cell design is described, the work lacks concrete guidelines for the iterative decisions involved in the decision-making process. As a result, the work serves as a general framework but is not readily applicable to real industrial cases. Shifting to task analysis, Gualtieri et al. [19] presented an algorithm for evaluating the feasibility of converting a manual assembly system to a collaborative process, also discussing numerous related works. The method emphasizes optimal task allocation between human and robot but provides limited guidance on essential pre- and post-allocation steps, such as task preparation and the development of a collaborative workflow, both of which are crucial for real-world implementation. Similarly, JC Mateus et al. [20] developed a framework for process analysis, providing guidelines for task distribution based on process constraints. This work develops the collaborative process starting from Computer Aided Design (CAD) models and adopts a linear approach, which may not adequately capture the inherently iterative nature of the design process. Furthermore, it does not address the final structure of the parallelized workflow or the layout of the workspace, both of which are essential for a comprehensive collaborative cell design. Then, Delle Mura et al. [21] introduced an algorithm for balancing human–robot collaboration in assembly lines with multiple operators. While these works, like many others in the literature, provide valuable insights into their respective areas, they do not offer a comprehensive overview of the overall design problem and approach. In addition, they do not include practical implementation tools, such as software recommendations or step-by-step procedures. As a result, non-experts aiming to apply current methods often need to combine multiple methodologies to cover all relevant aspects of the problem.

Building on the previous considerations, and with the aim of addressing the identified gaps, this paper provides the following novel contributions:

1. **Engineering method and tool** for designing collaborative workstations. The proposed workflow includes multi-domain aspects (i.e. assembly task analysis and allocation, cell and pallet layout, ergonomic assessment, commercial component selection, robot programming and simulation), promoting an integrated, general, and scalable approach applicable to diverse industrial scenarios.
2. **Validation of the proposed framework** on two industrial case studies, namely a worm gearbox and a gear pump, demonstrating its effectiveness in optimizing real-world scenarios. These case studies, purposely selected to represent various types and levels of assembly complexity, provide practical feedback on the proposed methodology, also highlighting the benefits of collaborative design. As a part of this validation, the developed assembly processes are replicated on a physical research cell.
3. **Open source dataset** related to the physical prototyping and testing of the implemented processes, shared to ease further developments and comparisons. The material includes flowcharts detailing the process sequences, robot programs and demonstration videos.

In the present work, all the experimental activities are conducted on a prototype cell established in the university lab. The cell is equipped with an ABB GoFa CRB 15000 cobot, though the approaches described are generally applicable and can be implemented with any other setup. Similarly, the virtual prototypes are created using Siemens Process Simulate, selected for its versatility and ability to conduct robotic and ergonomic simulations. In any case, designers can adopt alternative software without affecting the overall methodology.

The remainder of the paper is structured as follows: Section 2 provides an overview of the proposed design framework, detailing all steps and evaluation loops. Section 3 describes the adopted experimental setup. Section 4 presents the practical application of the methodology on two industrial case studies. At last, Section 5 provides a summary of findings and concluding remarks.

2. Proposed design framework

The proposed methodology aims to identify a viable and efficient design solution for the collaborative assembly of industrial products by integrating the interaction between human operators and cobots into existing processes [22,23]. Examples of such products can be found across various sectors, such as electronics (e.g. printed circuit boards or device assembly), automotive (e.g. component pre-assembly), and the medical sector (e.g. assembly of sterile healthcare components). With reference to Fig. 1, the framework consists of three main phases, each of them divided into specific sub-steps and evaluation routines. These

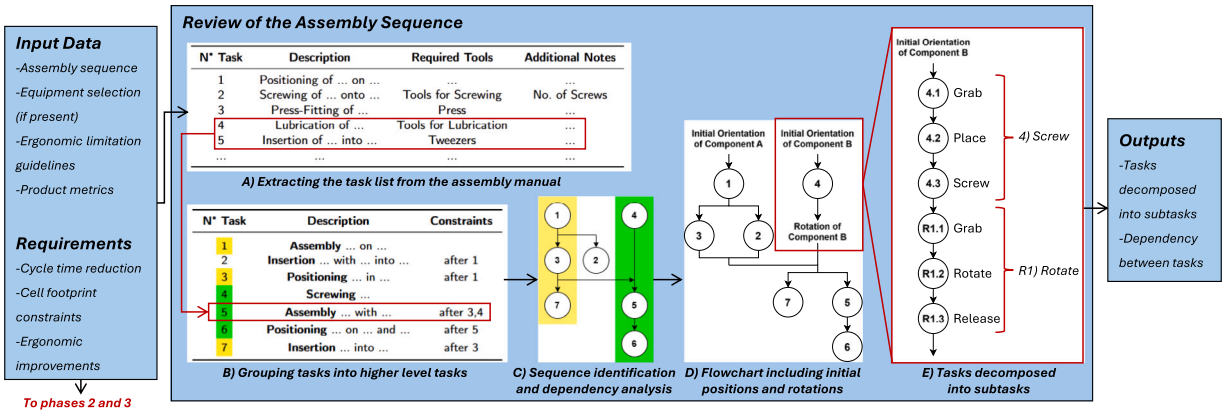

Fig. 2. Schematic representation of Phase 1 - Assembly task analysis. Steps A to E process the input assembly manual and generate the output assembly sequence, highly parallelized and divided into subtasks.

allow the progressive definition of the optimal configuration, tailored to meet case-specific requirements and performance optimization criteria. Starting from the specifications outlined in the assembly manual of the industrial product (provided by the producer), the iterative evaluation loops facilitate a detailed study of existing assembly operations, identifying critical points and opportunities for improvement. The procedure then moves to task analysis and allocation, considering both technical and ergonomic aspects. Once the collaborative sequence is defined and the workload is balanced between the operator and the cobot, the cell workspace is configured. The procedure ends with the virtual prototyping and simulation of the workstation, where the final quality checks are performed.

In the following Sections, each phase will be closely examined, analyzing the required inputs, operational steps to be implemented, and expected outputs.

2.1. Phase 1 - Assembly task analysis

This phase focuses on reviewing and reorganizing the assembly process to produce a newly structured task list, which will be used as input for Phase 2. Fig. 2 presents a detailed schematic of these activities, highlighting their inputs, outputs, and intermediate steps. The overall structure is divided into two main blocks: *Input Data and Requirements* and *Review of the Assembly Sequence*. The first block serves as a preparatory step, gathering all the necessary information, including:

- The assembly sequence extracted from the product assembly manual.
- The cell equipment, if preliminarily fixed by the client (e.g. robot, grippers, tools, interfaces, etc.).
- The recommended ergonomic limits, to be determined from the relevant standards based on the activities performed during the process. In case of manipulation tasks, an upper threshold of 23 kg (male) and 15 kg (female) is to be considered to mitigate the risk of musculoskeletal disorders [24].
- The product metrics, such as mass, dimensions, shape and surface properties for each component to be manipulated during the process.

The industrial requirements typically include cycle time reduction, adherence to cell footprint constraints, and ergonomic improvements.

The second block takes as input the original assembly sequence and, through a series of logical steps (from A to E in Fig. 2), generates a new parallelized assembly process, consisting of subtasks that enable the application of the classification algorithms proposed by this methodology and discussed in Section 2.2. In particular, the following steps are performed:

Step A is dedicated to extract the original sequence of tasks, which are systematically organized to ensure a comprehensive understanding of the overall workflow and the correct execution order. The elaborated list includes for each task: (i) a brief description, (ii) the tools required and (iii) any significant note (e.g. specific part orientation or multiplicity). This approach allows for a clear identification of the connections between components and the actions required for their integration, thereby simplifying the understanding of the entire assembly process.

Step B analyses each task in the list and groups more tasks into higher level tasks. To compensate for the information lost during this simplification, it is necessary to define and formalize the assembly constraints, namely to specify which task takes priority in execution with respect to others. Writing the constraints in this format identifies series of dependent tasks and their internal sequencing. In the example provided in Fig. 2, these sequences are represented by 1–3–7 and 4–5–6. Single tasks that are not part of any sequence (e.g., 2) will also be treated as a sequence. By organizing the task sequences, critical points are identified, which also facilitate the subsequent phase of task parallelization between human and robot (see Section 2.2).

Step C generates the visual flow diagram by arranging the previously identified sequences in different columns, all aligned at the top. The logical dependencies between tasks of different sequences are then incorporated by shifting the tasks downward according to their execution order. Conceptually, the upper part of the diagram represents the initial tasks in the assembly process, while the lower part shows the tasks that follow later.

Step D introduces the orientations of the key components during the process into the diagram. This can be done by referring to information extracted during **Step A**, namely by performing a critical review of the instructions provided on the product manual, aimed at optimizing the process sequencing.

Step E involves breaking down all the tasks of **Step D** into their respective subtasks.

The output of this block is an information-rich assembly process, structured as a sequence of well-defined, standardized, and unambiguous subtasks.

2.2. Phase 2 - Design of human-robot interaction

This phase involves classifying all subtasks and assigning them to the human, the robot, or both in a collaborative manner. The general structure of this phase, illustrated in Fig. 3, consists of three blocks: *Task Classification*, *Task Allocation*, and *Workspace Design*. As visible from the schematic, the second and third blocks are part of an iterative process that also extends into the subsequent Phase 3. During Phase 2, the identification of the equipment required to set up the cell is finalized, in cases where it has not already been explicitly fixed by the client.

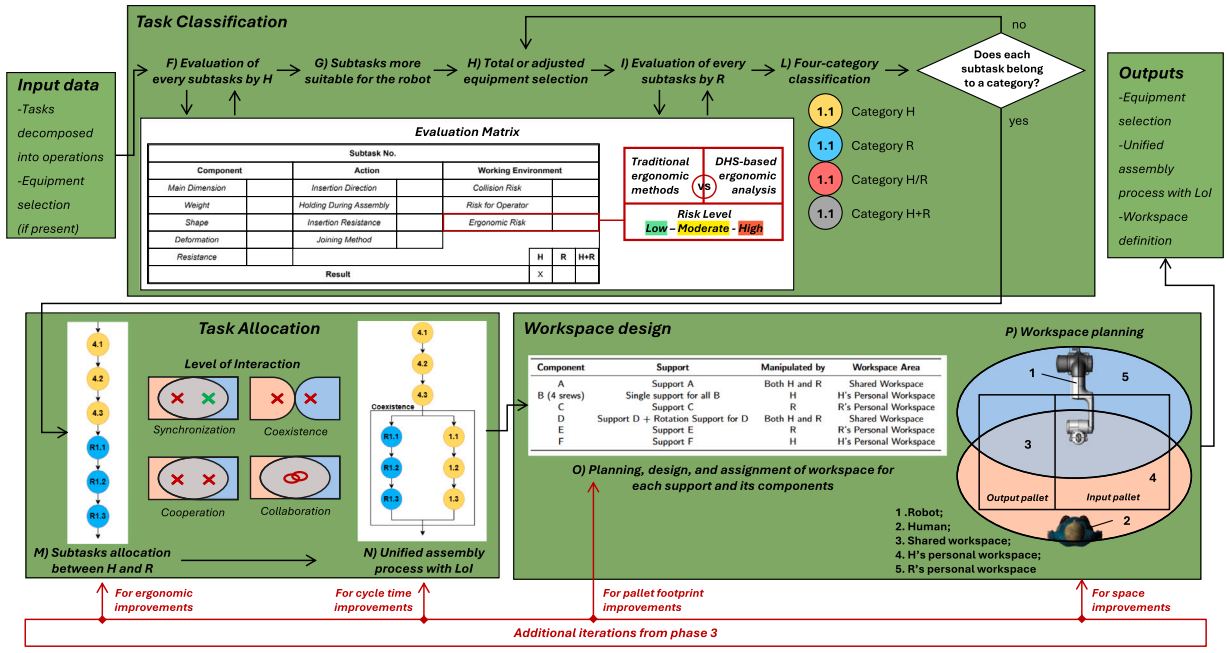

Fig. 3. Schematic representation of Phase 2 - Design of human-robot interaction. Steps F to L classify each subtask of the parallelized assembly process into four categories: H, R, H/R and H+R. Steps M and *N* unify the process by assigning each subtask to H or R and introducing the LoI. Steps O and P define the human and robot workspaces, providing the pallet design as output.

2.2.1. Task classification

The *Task Classification* block takes as an input the previously detailed subtasks (i.e. the output of Phase 1) and assigns each of them to a specific category, namely: (i) human only (→H), (ii) robot only (→R), (iii) human or robot (→H/R), or (iv) human with robot (→H+R) [25]. For this purpose, an evaluation matrix has been defined, as shown in Fig. 3, to assess each subtask from both the human and robot perspectives (**Step F** and **Step I**, respectively). This approach, originally introduced by Malik and Bilberg [26] and here adapted to the proposed methodology, is based on a set of attributes, each of which can be further divided into multiple factors. These factors enable the analysis of specific and relevant aspects of the subtask into exam, providing a clear indication of whether such subtasks can be performed by the human and/or the robot. In the proposed framework, the following attributes (and related factors) are considered:

1. Component (physical characteristics)
    - **Main dimension**: represents the component dimension(s) relevant to grasping.
    - **Mass**: indicates the mass of the component.
    - **Shape**: describes the geometry of the component and its level of symmetry.
    - **Deformation**: refers to the component deformability during handling.
    - **Resistance**: measures the fragility of the component and its vulnerability to damage during manipulation.
2. Action (type and complexity)
    - **Insertion direction**: it refers to the direction of component insertion or manipulation. Compared to a horizontal approach, vertical insertion is preferable for both humans and robots as it benefits from the assistance of gravity.
    - **Holding during assembly**: it refers to the need to hold down the component, maintaining its position or orientation either before or during the tasks.
    - **Insertion resistance**: refers to the resistance encountered during insertion, which is determined by the degree of fit between two components, defined in terms of tolerance. Excessively tight tolerances would require the robot to have highly accurate detection mechanisms, increasing complexity and cost, whereas this task is simpler for human operators.
    - **Joining method**: includes fastening and joining components through methods such as screwing, gluing, or bending. The more complex the assembly action, the greater the overall task complexity.
3. Working environment (human–robot workspace and ergonomics)
    - **Collision risk**: it assesses whether the use of a collaborative robot reduces the risk of collisions or enhances safety within the workspace.
    - **Risk for operator**: it considers the presence of components with sharp edges or burrs, use of power tools or tools with rotating parts, increasing the risk of accidents and injuries for the operator.
    - **Ergonomic risk**: it assesses the risk to develop musculoskeletal disorders (MSDs) by evaluating the nature of human activity, considering prolonged awkward postures or continuous movements, frequent bending or twisting, forceful exertions. The risk level is judged as low, moderate or high.

Among these, the ergonomic assessment factor is used to identify subtasks that are ergonomically unsuitable for assignment to a human operator [27]. At this stage of the methodology, only physical ergonomics is considered, while cognitive and organizational aspects will be addressed later. In this way, low-risk subtasks can be safely assigned to a human operator, moderate-risk subtasks should be limited whenever possible, and high-risk subtasks pose a possible threat to the physical health of the operator and must therefore be avoided or assigned to the robot.

The considered ergonomic methods and indices are divided into: (i) postural methods, which rely on the analysis of human postures assumed and the nature of actions (static or dynamic, intermitted or repetitive, if lifting loads), and (ii) load-handling methods, which

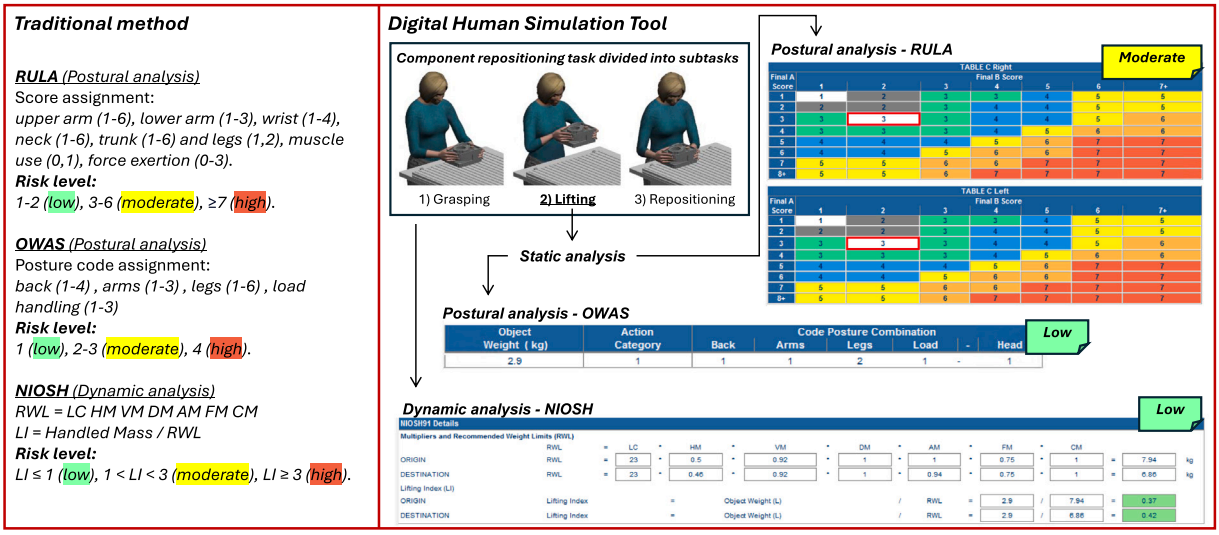

Fig. 4. Example of ergonomic assessment during assembly tasks: traditional calculation vs. analysis with human digital simulation tools (Process Simulate).

involve the dynamic analysis of handling tasks to specifically examine the movements and timing of work as the body interacts with loads. One of the most commonly used primary methods to analyze postural stress during work activities is the Ovako Working Posture Analysis System (OWAS). It focuses on whole-body postures that workers adopt while performing tasks and assesses the associated risks of MSDs, helping to quickly identify postures that may cause physical strain and require ergonomic intervention [28,29]. Each posture is categorized using a 4-digit code, where each digit expresses a score based on the angles of the body parts (neck, back, arms, and legs). The scores help determine whether a posture is potentially risky: back posture (1 to 4), arm position (1 to 3), leg position (1 to 7), load handling (1 to 3) [30]. Once the codes are identified, the OWAS risk matrix is used to assign a risk category: 1 (low), 2–3 (moderate) and 4 (high). In order to specifically focus on the upper limbs, which are the most involved in assembly operations, the mostly used postural method is the Rapid Upper Limb Assessment (RULA), which addresses the risk of MSDs in the upper limbs by analyzing specific postures, forces, and movements involved in a task. It is especially suited for analyzing intermittent movements, which are particularly common in assembly operations [31]. The method is based on assigning a score to each musculoskeletal region involved: upper arm (from 1 to 6), lower arm (from 1 to 3), wrist (from 1 to 4), neck (from 1 to 6), trunk (from 1 to 6), legs (1 or 2), considering additional scores in presence of muscle use (0 or 1) and force exertion (from 0 to 3). By comparing these values with lookup tables, the corresponding risk level is determined: 1–2 (low), 3–6 (moderate) and ≥7 (high). For more information, the interested reader should refer to [32,33]. As for dynamic load-handling analysis methods, the NIOSH (National Institute for Occupational Safety and Health) lifting equation is widely used to assess the risk of musculoskeletal disorders related to manual lifting tasks. As discussed in [24,34], the evaluation begins with calculating the Recommended Weight Limit (RWL), obtained by multiplying the load constant (23 or 15 kg) with a set of multipliers describing the lifting conditions (i.e. horizontal distance, vertical distance, lifting distance, asymmetry in task execution, frequency of action, quality of gripping). The ratio between the mass of the object to be handled and the RWL (i.e. Lifting Index—LI) allows to define the related risk: $LI \leq 1$ (low), $LI > 1$ (moderate) and $LI > 3$ (high). NIOSH equation is dedicated to the lifting actions, that are the most frequent in assembly operations; similar indexes, such as the Snook and Ciriello tables (see [35]), can be used for different types of activity (i.e, pushing, pulling, lowering, carrying).

The ergonomic evaluation can be performed using either traditional methods or modern digital simulation tools, as illustrated in Fig. 4. The traditional method relies on user observation and recording and the following activity analysis by applying formulas according to the ergonomic methods (i.e. OWAS, RULA, NIOSH) to determine the related risk level. It is time-consuming, labor-intensive, and lead to inconsistent results due to the experts' subjectivity. Comprehensive guidelines for selecting and applying these formulas, alongside with various examples, are provided in [27,36,37]. To streamline the evaluation process and enhance accuracy and repeatability, digital human simulation tools are recommended. These multi-domain software platforms enable the creation of virtual production environments that accurately replicate human tasks and their interactions with all relevant devices, recently including robots and cobots. In this work, the ergonomic analysis is conducted using Process Simulate (Siemens Tecnomatix), though Delmia (Dassault Systèmes) and Ramsis (Human Solutions) are other viable alternatives. While the use of these tools is recommended for virtual modeling, it is not mandatory, as ergonomic evaluations can be still addressed manually using the well-established formulas. Today, such platforms integrate the most widespread ergonomic methods to provide a comprehensive and realistic simulation and analysis of the work environment and related processes, reducing manual effort and fastening the evaluation. In Fig. 4, an example of ergonomic risk assessment conducted using Process Simulate is shown. A generic component repositioning task has been divided into subtasks, with a specific focus on subtask 2 (lifting). The two postural analyses, performed with OWAS and RULA, do not indicate any specific postural risk. After that, the full task analysis is conducted using the NIOSH method to detect specific load-handling risks that postural analysis might have missed, resulting in a low-risk level.

Once the evaluation matrix is fed with all information, **Step F** determines whether each subtask can be executed by the human or not. This is accomplished by analyzing each factor individually, providing a clear understanding of the complexity and key characteristics of the required actions. The subtasks that are more suited for robot assignment are listed together in **Step G**. With this input, **Step H** consists of the total or partial selection of the necessary cell equipment (robot, devices, and related tools). During **Step I**, a second evaluation of all subtasks is performed from the robot perspective. It is important to emphasize that this second analysis must be conducted for every subtask, including those that can also be performed by the human, to identify subtasks belonging to the H/R category. At last, **Step L** assigns each subtask to a specific category (H, R, H/R or H+R). To add this information to the

Table 1
LoI classification based on workspace and task types. In the table, "Collab.", "Coop.", "Sync." and "Coex." respectively indicate collaboration, cooperation, synchronization and coexistence.

		TASK		
		Shared	Non-shared	
			Same time	Different times
Workspace	Shared	Collab.	Coop.	Sync.
	Separate	–	Coex.	–

previous flowchart from Phase 1, a color legend is utilized, as visible in Fig. 3.

If all subtasks have been assigned to a category, the process can advance to the next block, otherwise it returns to **Step H**, where equipment selection is further refined to ensure that all subtasks are covered. The distribution of subtasks among the categories R, H/R, or H+R, compared to those assigned to H, provides valuable insights into the level of human–robot collaboration achievable within the process. If greater robot assistance is desired, more advanced or alternative equipment must be selected to increase the number of tasks falling into robot-inclusive categories (R, H/R, or H+R). This classification, along with the refined equipment selection, represents the final output of this block.

2.2.2. Task allocation

The *Task Allocation* block is the first of four stages that comprise the iterative cycle for process optimization, as shown in the overview of Fig. 1. From this point onward, every decision can be reviewed based on the results and considerations from subsequent steps. The objective of this block is to create a rule-based allocation of tasks to define in a systematic way if a task should be assigned to H (human) or R (robot) [38]. This step serves as the foundation for the subsequent steps about workspace spatial organization and virtual prototyping.

Specifically, during **Step M**, an initial task allocation is carried out based on the following principles:

- If all subtasks within a specific task are classified as H/R, the entire task is initially assigned to either H or R. Specifically, if at least one subtask is classified as H, the entire task is assigned to H. Similarly, if at least one subtask is classified as R, the entire task is assigned to R. In cases where subtasks are a mix of both H and R classifications, it may be necessary to divide the task, assigning portions of it to H and R as appropriate. Finally, if any subtask is identified as medium-risk during the ergonomic analysis, the entire task is assigned to R.
- If a task includes a subtask classified as H+R, that subtask is retained as collaborative, while the neighboring subtasks are preliminarily assigned based on their classification.
- In the most complex case, involving a mix of all categories, a preliminary allocation is performed based on the classifications from **Step L**.

Next, **Step N** consolidates the assembly flow according to two rules, i.e.: (i) tasks and subtasks graphically arranged in different (parallel) columns in **Step M** (derived from the output of **Step D**, see Fig. 2) can be executed simultaneously, (ii) only tasks or subtasks assigned to different actors (H or R) can be effectively performed at the same time (e.g., R cannot execute two tasks simultaneously) [39]. In addition to the task sequencing, the revised workflow includes indications of the Levels of Interaction (LoI) between H and R [40]. These levels have been identified starting from the following possible scenarios:

1. Both H and R are stationary (not relevant for interaction).
2. H is moving, and R is stationary (fully human controlled).
3. H is stationary, and R is moving (fully robot controlled).
4. Both H and R are moving.

Then, a distinction has been made between shared tasks (H+R) and non-shared tasks (H or R), executed either at the same time or not. A further distinction considers the workspace, as detailed in Fig. 3, differentiating between tasks executed in a shared workspace and those executed in separate workspaces. By analyzing all possible combinations of interest, the following LoI are determined [8,40]:

- **Synchronization**: H and R execute non-shared tasks at different times within a shared workspace.
- **Coexistence**: H and R execute non-shared tasks simultaneously in separate workspaces.
- **Cooperation**: H and R execute non-shared tasks simultaneously within a shared workspace.
- **Collaboration**: H and R execute a shared task within a shared workspace.

For a better visualization of these combinations, please refer to Table 1. The workflow of **Step N**, enriched with the information regarding the LoI, represents the output of this block and will be utilized in subsequent blocks to design the workspace.

The continuation of the iterative cycle will generate a first-attempt version of the cell and a preliminary virtual simulation of the entire assembly process. If inconsistencies arise in meeting the prescribed requirements, the iterative cycle will loop back to this block, allowing to development of an improved workflow. This may occur if further ergonomic improvements are needed, requiring adjustments at **Step M**, particularly for tasks previously identified as moderate or high risk during the ergonomic evaluation. Assigning these tasks to the robot can help to alleviate the human workload. Such adjustments will also impact **Step N**, necessitating a recalculation of the corresponding LoI. Conversely, if a shorter cycle time is desired, modifications will begin at **Step N** with the goal of optimizing task parallelization.

The ultimate goal is to achieve a solution that meets the designer objectives while minimizing invasive changes from the previous cycle. This characteristic of iterative cycles with expanding scope is particularly evident in this block and becomes even more prominent in subsequent stages. This form of task allocation is commonly referred to as static task allocation and is typically applied during the design phase of collaborative processes, which is the focus of this study. Since it is intended for structured planning based on expected conditions and predefined task sequences, it is often complemented by dynamic task allocation during the operational phase, where tasks may need to be reassigned in response to unforeseen events or operator variability. Dynamic allocation leverages real-time data from sources like sensors, vision systems, wearable devices, or decision models trained using artificial intelligence algorithms to continuously adapt the process as required. While the proposed framework is not intended for real-time operation monitoring, its modular structure supports iterative updates, making it adaptable to insights gained during process validation and physical testing. For details regarding dynamic task allocation, the reader can also refer to [41–44].

2.2.3. Workspace design

In this block, the positions of human and robot within the workstation are established, along with the allocation of shared and non-shared workspaces [45]. The design of the input/output pallets, as well as their internal layout, namely the positioning of parts and related supports within the prescribed areas, are also determined. The block is divided into **Step O** and **Step P**. The former is dedicated to extracting and organizing information received from **Step N**, while the latter focuses on implementing the design considerations.

After careful evaluation of the unified assembly sequence, **Step O** determines the supports needed for each component involved, namely individual parts but also subassembly requiring a support surface. These supports must also be properly located on the pallets. In particular, if a support holds an item manipulated exclusively by the human or robot, it will be placed in their respective dedicated workspace. Conversely,

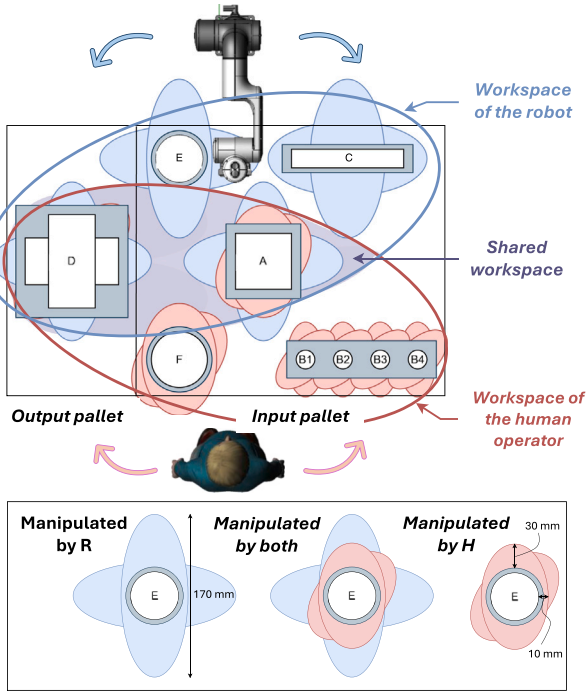

Fig. 5. Example of cell workspace design: human–robot relative position, definition of shared/non-shared workspaces, manipulation areas, and input/output pallet identification.

in case the support holds a component utilized in a shared task (H+R), it will be placed in the shared workspace. The LoI provides additional guidance in defining the appropriate workspace zone. When the action involving a specific support falls under collaboration, cooperation, or synchronization, this will be placed in the shared workspace. An example of list of supports and related assignments is shown in Fig. 3. Once the list is finalized, a detailed 3D solid model is generated in CAD environment for each support, which can be further refined in the following passages.

Step P, illustrated in Fig. 5, involves creating the layout for the work pallets and defining the shared and non-shared work zones. To achieve this, the footprints of both the supports and their accommodated components are extracted from the CAD model. When a support functions as a base, transit point, or rotational guide, the footprints of all interacting components are considered. The most conservative footprint, represented in gray in Fig. 5, is then selected for each item to ensure proper space allocation.

Next, the manipulation area [9], namely an offset extending from the center of the support and representing the space occupied by the human hand or robot tool during the manipulation of the object (e.g. grasping, releasing or reorienting actions) is evaluated. In particular, if the component under consideration is manipulated by the human operator, two possible manipulation areas are added. The first area includes an offset of 30 mm vertically and 10 mm horizontally on each side (based on practical grip and release trials), while the second has the same values but is tilted at 45° to simulate an alternative grip on the component. In the case of robot manipulation, the footprint area occupied by the robot during component handling must be derived from the manual of the attached tool (selected during **Step H**). Also in this case, two areas have been considered, one vertical and one horizontal. Alternatively, a circular manipulation area can be used to remain more conservative and thus consider infinite manipulation configurations. At last, if a component is manipulated by both H and R, all zones must be overlapped. To facilitate the distinction between H and R areas, different colors are recommended (e.g. light blue and red, see Fig. 5).

Once these areas have been defined, the components are divided into the three workspaces to be designed [46]: the shared workspace, the human or the robot dedicated workspaces. During this assignment, based on the output list of **Step O**, the relative position of H and R is also to be determined, either based on case-specific requirements or as an initial attempt. Components must be placed close to each other, adhering to the boundaries set by the manipulation areas and respecting the division of the workspaces. An input pallet must then be identified, containing the components to be assembled, along with an output pallet, on which the completed assembly will be placed prior to exit the cell.

As mentioned earlier, in Phase 3 an initial virtual prototype of the cell and a simulation of the entire assembly process will be developed. In case the cell space requirements are not met, adjustments will be made to **Step O** or **Step P**, leaving the results from the previous steps unchanged. These modifications may involve altering the design or the number of supports, possibly integrating them to reduce their quantity and enabling the reuse of the same support for multiple subtasks.

2.3. Phase 3 - Virtual prototyping and optimization

This phase is dedicated to virtual prototyping and simulation to assess cell performance and potentially finalize the iterative design cycle. With reference to Fig. 6, it comprises two main blocks, namely *Virtual Model* and *Performance and Ergonomic Analysis*, which are detailed in the following sections.

2.3.1. Virtual model

By including all the information from Phase 2, the virtual model incorporates the complete set of equipment for both human and robot activities, the design workspace and the unified assembly sequence with the indication of the LoI. After importing all necessary CAD models (equipment from *Input Data* and **Step H**, and pallets and supports from **Step P**), **Step Q** focuses on replicating the cell environment within the simulation software. This can be done using either proprietary tools specific to the selected robot model (e.g. ABB RobotStudio, Fanuc RoboGuide) or a general-purpose platform like Process Simulate. Proprietary tools offers high-fidelity simulations of robot behavior as they incorporate the exact replica of the software running in the real controller. However, these tools often have limited integration capabilities for human modules, which are essential for this assessment. As a result, Process Simulate may be considered a convenient and more practical option for accurately modeling both human and robot activities, including all the needed interactions [7,47].

During **Step R**, the collaborative assembly process outlined in **Step N**, is implemented. This includes programming the human and robot tasks (e.g. movements, actions, object attach/detach, signals, station logic) and organizing the entire workflow. The main modeling steps include:

1. Create new mechanisms and provide them with appropriate logic (e.g. commercial gripper).
2. Define and save the target points for human and robot movements.
3. Refine the spacing values between approach targets for grabbing and releasing components.
4. Create the paths to be followed by both H and R and assign proper speed values.
5. Define signals and develop control logic to manage interactions and signal exchange.
6. Define process sequencing through detailed robot programming.

Regarding the speed assignment, a significant portion of the literature focuses on interaction safety [11,48], particularly the appropriate speed limits a cobot should adhere to when operating near a human operator [38]. It is important to note that the maximum speed of a cobot is often limited by safety regulations [10], such as those

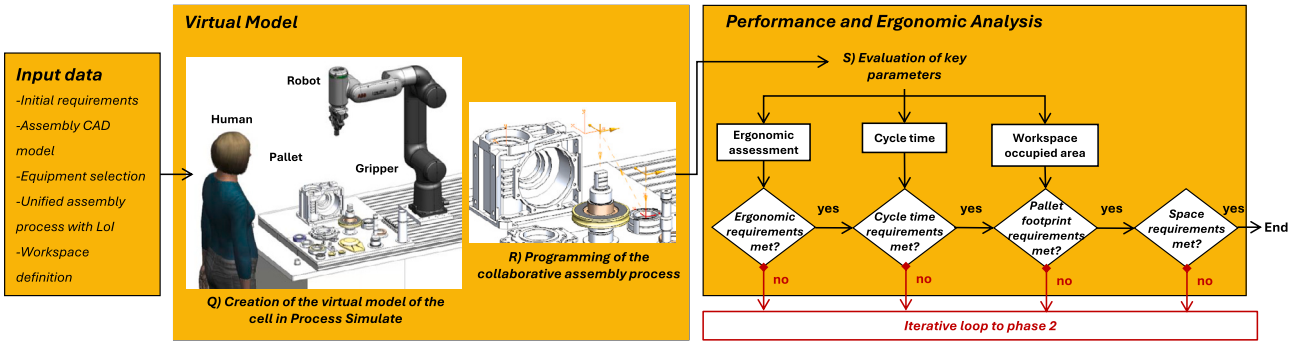

Fig. 6. Schematic of Phase 3 – Virtual prototyping and optimization. Steps Q to S use previously defined inputs to build a 3D simulation model and run the collaborative process for final validation. An iterative loop enables design refinements in earlier blocks.

outlined in ISO/TS 15066. According to this standard, the maximum allowable speed for a cobot operating near a human is approximately 250 mm/s. However, this limit should be further adjusted on a case-by-case basis, considering multiple factors such as the characteristics of the component being handled. About human speed, realistic values can either be retrieved from databases or assigned based on preliminary testing.

The output of this block is a virtual collaborative cell that incorporates all key components, accurately replicating the assembly process as defined by the proposed methodology up to this point.

2.3.2. Performance and ergonomic analysis

The last block is dedicated to the evaluation of the entire assembly process. As shown in Fig. 6, the following data can be calculated during simulation:

- Ergonomic risk scores according to the selected ergonomic methods (OWAS, RULA and NIOSH).
- Cycle time (overall and related to each single task/subtask).
- Cell footprint and occupied space area.
- Additional data (e.g. path feasibility, collision checks, robot energy consumption).

Based on the performance of the virtual cell, a decision can be made to either further refine the model or consider the results satisfactory and conclude the design. As visible in Fig. 6, if the requirements are not met, iterative loops will be initiated respectively in **Step M** (ergonomics), **Step N** (cycle time), **Step O** (pallet redesign) and **Step P** (space allocation). This checkpoint structure allows each block to function independently or as part of the overall methodology, driving the design process in a systematic way.

The methodology is flexible, adapting to a wide range of case studies and providing tailored, optimized solutions for various scenarios and practical applications. In cases where specific goals are not defined, the methodology ensures general optimization. This approach fosters the development of an effective collaborative assembly process by leveraging the complementary strengths of humans and robots.

3. Experimental setup

This section presents the experimental setup used to validate the design methodology. The tests are conducted within a collaborative cell installed at the University facility. The cell, shown in Fig. 7, includes the following equipment:

- An ABB GoFa CRB15000 6-axis cobot with a maximum payload of 5 kg, maximum reach of 1050 mm, and maximum end-effector speed of 2.2 m/s [49]. The cobot is controlled by an OmniCore C30 and programmed using the RAPID language in RobotStudio.
- A RobotiQ 2-Finger 85 electric gripper, a highly versatile tool suitable for a wide range of robotic applications. The 2-Finger gripper has a total mass of 925 g and is equipped with a single actuator that controls the opening and closing of the jaws, allowing for intermediate positions. The device is connected to the OmniCore C30 via the scalable IO interface and is thus commanded via specific instructions in the RAPID code. In particular, its driver module allows the programmer to specify both position and gripping force, to be tuned based on the object to handle (mass and surface properties). By exploiting redundant kinematics in the jaw mechanism, the gripper can perform both encompassing and parallel grips (see detailed schematic in Fig. 7). It also supports internal gripping, in addition to the standard external mode. The maximum opening is 85 mm.
- A Laptop PC with RobotStudio for robot programming and process monitoring. It shall be noted that the robot program is initially generated through the Process Simulate post-processor after simulation, and then fine-tubed in RobotStudio before being downloaded to the OmniCore C30 controller.
- A light device featuring 3 different colors (acting like a traffic light system), used to provide real-time visual feedback to the human operator. The device is controlled and activated by the OmniCore C30 to indicate the robot status during production. The green light indicates that the robot is ready, the yellow light indicates that the robot is actively performing a task (busy), whereas the red color alerts the operator to errors and consequent process abort.
- A push button used as human-to-robot interface (robot input) to send enabling requests or notify the completion of a human task, thereby facilitating correct process sequencing through event-based logic. In the RAPID script, the received digital input (button pressed) is managed through a dedicated procedure implementing *WaitDI* commands.
- A fixed-base table (2.2 × 0.85 m, 1 m height) that serves as the platform for mounting all the cell devices.
- A set of tools for the operator (i.e. gloves, clamps, hex keys) arranged on a secondary pallet. These must be selected based on the product being assembled.

As visible in Fig. 7, in the current cell configuration the operator is located in front to the robot, exploiting the table longitudinal direction to optimize the robot installation and accommodate the pallets. Despite the specific test setup used in this work, it should be noted that the proposed design framework is applicable to any commercial equipment, which is to be appropriately selected during **Step H** in Phase 2.

4. Methodology validation

In this section, the methodology described in Section 2 is validated. Two industrial case studies have been selected for this purpose, characterized by a different level of complexity: (i) assembly of a gear pump

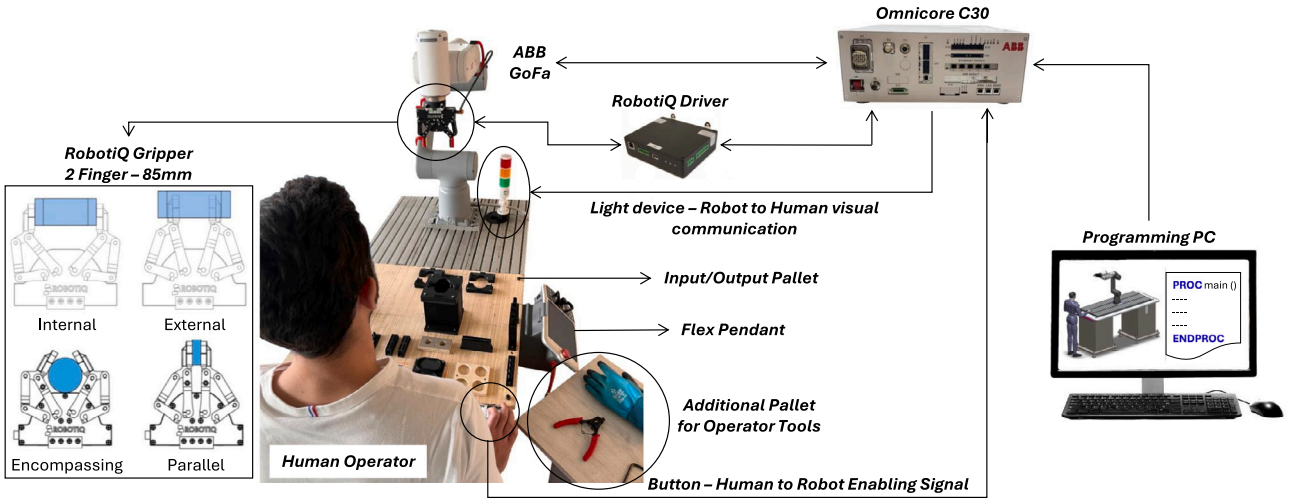

Fig. 7. Collaborative workstation used for validation: overview of the hardware and logical connections.

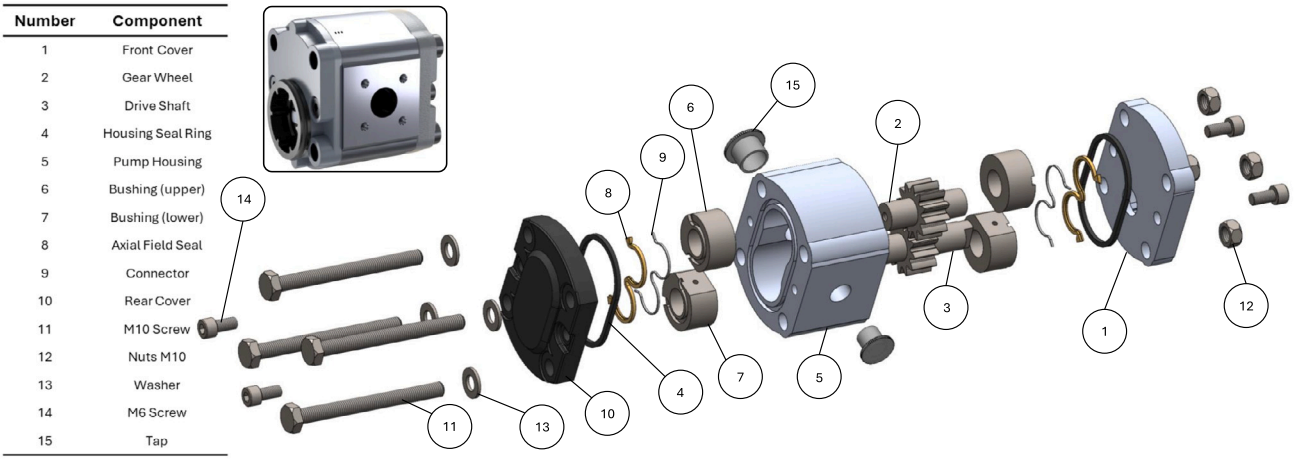

Number	Component
1	Front Cover
2	Gear Wheel
3	Drive Shaft
4	Housing Seal Ring
5	Pump Housing
6	Bushing (upper)
7	Bushing (lower)
8	Axial Field Seal
9	Connector
10	Rear Cover
11	M10 Screw
12	Nuts M10
13	Washer
14	M6 Screw
15	Tap

Fig. 8. 3D model of the gear pump and part list.

(BOSCH AZPF series) and (ii) assembly of a worm gearbox (Bonfiglioli W63 series). The gear pump serves as a first illustrative example, as it allows easy application of the methodology due to its simple component arrangement along a single functional axis. In contrast, the worm gearbox requires a more complex assembly procedure to efficiently mount its components, which need to be assembled along two perpendicular axes. By considering the experimental setup detailed in Section 3, the equipment is preliminarily fixed (as it could happen in an industrial setting) and only reviewed during Phase 2.

4.1. Case 1: Gear pump

The hydraulic pump under consideration consists of a pair of gears supported by bushings, a central housing, and two covers (front and rear). Fig. 8 presents the exploded view of the pump CAD model, along with a list of its components. To prevent fluid backflow to the intake area, the pump relies on tight tolerances between the gear teeth and the housing walls, along with pressure fields designed to press the bushings against the gears. All pressurized areas are enclosed with multiple seals to ensure fluid containment and maintain pressure. The high precision required during assembly, combined with the handling of seals, still necessitates human involvement in assembling this type of pump.

The input data consists of the assembly sequence (extracted from the manual), the equipment (fixed setup), ergonomic limits (15 kg, female user) and the product metrics. The model under consideration has a total mass of 2.5 kg and dimensions of 112.5 × 101 × 88 mm (bounding box: length, width, and height). The primary requirements focus on reducing cycle time and, where possible, minimizing tasks that involve reorienting the parts. While the maximum mass of 2.5 kg imposes minimal stress during these rotations, prolonged repetition can still engage the back and torso muscles.

4.1.1. Phase 1

From the original assembly sequence, the tasks related to component refilling (from bins or conveyors) and related quality checks have been removed, as in this validation it is assumed that the components arrive at the collaborative workstation already placed on a pallet and pre-checked. Additionally, the final oil adduction and quality tests on the assembled pump have also been removed. **Step A** is therefore the extraction of the main tasks required for the correct assembly of the pump, listed in Table 2.

Starting from this list, in **Step B** the information related to the same component has been grouped together, leading to the higher level list of tasks in Table 3. For example, task 1 and 2 in Table 2, referring to the rear cover, have been grouped into a single positioning task. The new list also specifies the constraints (task dependencies), defined by analyzing the requirements of each task for its completion.

With reference to Fig. 9, in **Step C** the identified series are arranged within a flowchart, and the remaining constraints are added to initiate

Table 2
Main task list extracted from the assembly manual of the gear pump. The list excludes component refilling, quality checks, final oil adduction and inspection of the completed assembly.

Step	Description	Required tools	Additional notes
1	Lubricate the pump housing cavity.	Lubrication	"Rear" side
2	Position the rear cover on the pump housing.		
3	Secure the rear cover to the pump housing with two M8 screws.	Screwing	
4	Rotate the pump housing.		"Front" facing up
5	Lubricate the pump housing cavity.	Lubrication	"Front" side
6	Align the bearing bushing M with F.		
7	Mesh the drive shaft with the gear wheel.		
8	Align the drive shaft and gear wheel with bearing bushing MF.		
9	Insert bearing bushing M into F.		
10	Insert bearing bushing MF into the gear.		
11	Insert the bearing bushing with gear and drive into the pump housing.		
12	Insert the supporting element.		"Front" side
13	Insert the housing seal ring.		"Front" side
14	Insert the axial seal.		"Front" side
15	Position the front cover on the pump housing.		
16	Secure the front cover to the pump housing with two M8 screws.	Screwing	
17	Rotate the pump housing.		"Rear" facing up
18	Remove the two M8 fastening screws.	Screwing	
19	Remove the rear cover.		
20	Insert the supporting element.		"Rear" side
21	Insert the housing seal ring.		"Rear" side
22	Insert the axial seal.		"Rear" side
23	Position the rear cover on the pump housing.		
24	Secure the rear cover to the pump housing with two M8 screws.	Screwing	
25	Rotate the pump housing.		Laterally
26	Position an M10 washer on the rear cover.		x4
27	Insert the M10 screw into the rear cover.		x4
28	Secure the M10 screw with a Nut10.	Screwing	x4
29	Rotate the pump housing.		"Rear" facing up
30	Tighten four M10 screws.	Screwing	
31	Insert the caps.		

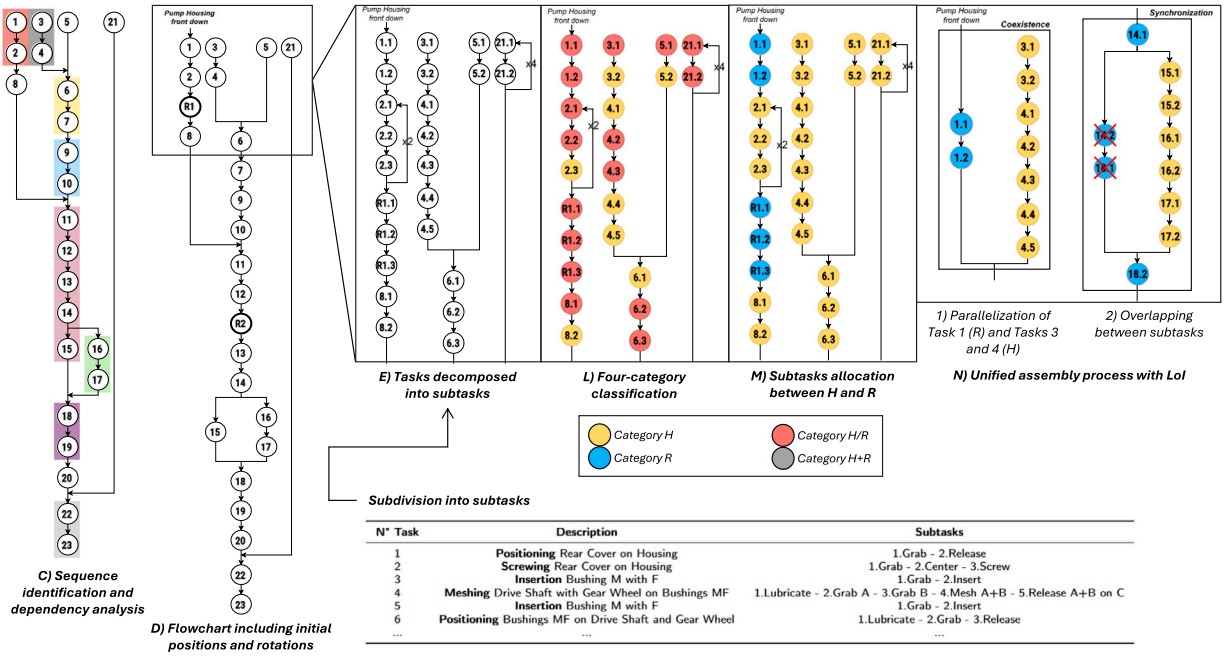

Fig. 9. Development of the collaborative assembly flow in the gear pump case. Steps C to E belong to Phase 1. Steps L to *N* are part of Phase 2, and are preceded by steps F to I (not shown in the image).

the creation of the new assembly process. Tasks 1–2 and 3–4 are independent and can therefore be performed in parallel, as can task 5. However, tasks 6–7 depend on the completion of task 5, so these are shifted below. This process is applied to all tasks.

The only component within the assembly for which the initial position is critical is the pump housing. **Step D** focuses on determining this initial position, which will influence all subsequent rotations. To minimize the total number of rotations, it was decided to position the housing with the front facing downward. This reduces the number of rotations from 4 to 2 throughout the process. **Step E** involves decomposing the newly created flowchart into subtasks by breaking each task down into its atomic actions. For example, the meshing of the drive shaft with the gear wheel was divided into lubrication, grasping the first component, grasping the second component, meshing, and

Table 3
List of higher-level tasks after Step B for the gear pump case.

Task	Description	Constraints
1	**Positioning** Rear cover on housing	
2	**Screwing** Rear cover on housing	After 1
3	**Insertion** Bushing M with F	
4	**Meshing** Drive shaft with gear wheel on bushings MF	After 3
5	**Insertion** Bushing M with F	
6	**Positioning** Bushings MF on drive shaft and gear wheel	After 5,4
7	**Insertion** Bushings with shafts in housing	After 6
8	**Positioning** Housing seal ring in housing	After 2
9	**Positioning** Axial seal in housing	After 7
10	**Insertion** Supporting element in housing	After 9
11	**Positioning** Front cover on housing	After 7,8,10
12	**Screwing** Front cover on housing	After 11
13	**Unscrewing** Rear cover	After 12
14	**Removal** Rear cover	After 13
15	**Positioning** Housing seal ring in housing	After 14
16	**Positioning** Axial seal in housing	After 14
17	**Insertion** Supporting element in housing	After 16
18	**Positioning** Rear cover on housing	After 15,17
19	**Screwing** Rear cover on housing	After 18
20	**Positioning** Washer M10 on rear cover	After 19
21	**Positioning** Nuts M10 on front cover	
22	**Screwing** M10 on housing	After 20,21
23	**Insertion** Caps	After 22

final positioning. Tasks involving multiplicities are indicated with a repeated loop.

4.1.2. Phase 2

During **Step F**, all the subtasks have been examined from the human perspective through the evaluation block described in Section 2.2. In this specific case study, given the reduced size and relatively low mass of all the parts, this evaluation has not identified any critical task for the human (**Step G**). However, the ergonomic assessment conducted in Process Simulate confirmed that among all tasks, special attention should be given to the reorientation of the pump housing, especially towards the end of the process, when almost all parts are mounted and the pump reaches approximately 2.5 kg. The RULA index, provided as output by Process Simulate, is equal to 3 for the rotations of the pump housing, while it never exceeds 2 for all other tasks. This suggests the need to reduce these reorientation tasks. Since the equipment was already fixed a priori, the process rapidly moved to **Step I** and **Step L**, where each tasks is assigned to one of the four categories: H, R, H/R, H+R. Although no task was classified as H+R, the number of subtasks assigned to categories R and H/R was deemed satisfactory. Therefore, it was decided to proceed without reiterating.

Following the guidelines in Section 2.2.2, in **Step M** the allocation was performed task by task, prioritizing the assignment of as many rotation tasks as possible to the robot. Although the number of subtasks assigned to H is greater than those assigned to R, it is important to note that the H subtasks are executed more quickly than those assigned to R. Additionally, the tasks assigned to R include those previously marked as "to be reduced" for human execution. By introducing the LoI, **Step N** led to the creation of a unified assembly flow. Referring to Fig. 9, the following examples illustrate the process:

1. Considering task 1, which is assigned to the robot, the question becomes: "What can the human do in the meantime?" Since tasks 3 and 4 are not dependent on task 1 and are already parallel to it, they were also placed in parallel in the updated flowchart. Given that these tasks occur in different workspaces simultaneously, the associated LoI is Coexistence. This approach was applied to all tasks, systematically determining which tasks could be executed in parallel while respecting their dependencies.
2. Subtasks 14.1 and 14.2 involve grasping the rear cover from the pump housing and releasing it onto the pallet, while subtasks 18.1 and 18.2 are the reverse, from the pallet to the pump housing. Assigning consecutive subtasks or tasks to the same actor, whether human or robot, may result in overlapping actions (as seen with 14.2 and 18.1). However, this overlap does not invalidate the method. The designer must address and resolve these overlaps during the virtual prototyping phase to ensure the assembly process remains efficient.

Based on the unified flow, **Step O** focuses on the design of the supports. Two auxiliary supports are introduced: (i) support for the rotation of the gear pump, (ii) support for the meshing of the shafts (part 2 and 3 in Fig. 8), before the insertion into the pump housing.

Finally, in **Step P** where the human is positioned 1 m in front of the robot, the component and support layout are designed in accordance with the guidelines reported in Section 2.2.3. The input pallet is placed to the operator's right (for right-handed users), while height-adjusted supports, such as the pump housing support and M10 screw holders, are positioned in front of or beside the operator to prevent interference during tasks. The shared workspace is shifted towards the operator to enhance accessibility and comfort. The shaft meshing support is vertically aligned with the insertion point, ensuring precision for this critical task. Lastly, the rotation supports are placed to minimize robot movement, reducing both travel distance and execution time. The resulting pallet layout is shown in Fig. 10, along with its physical prototype used during the final experiment (see Section 4.3).

4.1.3. Phase 3

Following the procedure outlined in Section 2.3, during **Step Q** the virtual model of the experimental collaborative cell has been created within Process Simulate. The complete CAD model of the pump (see Fig. 8) and of the pallets is then imported, allowing the precise programming of all human and robot movements (**Step R**). From the analysis of the created virtual process, conducted within **Step S**, the following conclusions can be drawn:

1. The requirement to reduce reorientation tasks was met, as the number of rotations decreased from four (original assembly) to two (collaborative assembly), both of which were assigned to the robot. Additionally, the LI index from the NIOSH equation conducted in Process Simulate never exceeds a value of 1.
2. An overall cycle time reduction of 8.8% was achieved, stepping from 5 min and 17 s (original process) to 4 min and 49 s (simulated collaborative process). For the evaluation of the original cycle time, two approaches have been followed. The first approach employed the Boothroyd & Dewhurst method [50], a structured and systematic methodology for estimating product assembly times, based on specific parameters and standardized tables. The script for time calculations is available in the supplementary material section of this paper. This method produced a manual cycle time of about 5 min. The second approach involved the manual replication of the original assembly operations. A series of practical tests (see Section 4.3) resulted in an average assembly time of 5 min and 17 s.
3. To achieve further improvements on cycle time, one should return to **Step N** and explore additional opportunities to parallelize the tasks. By observing the simulation, a possible example is subtask 12.1, parallel to task 11 performed by the robot, which was completed by the human much faster than expected, swapped with task 21, which had a higher time consumption. The change made in **Step N** has not required modifications to the subsequent steps, but led to a further improvement in cycle time, reducing it to 4 min and 40 s (time reduction of 11.7% compared to the original process).

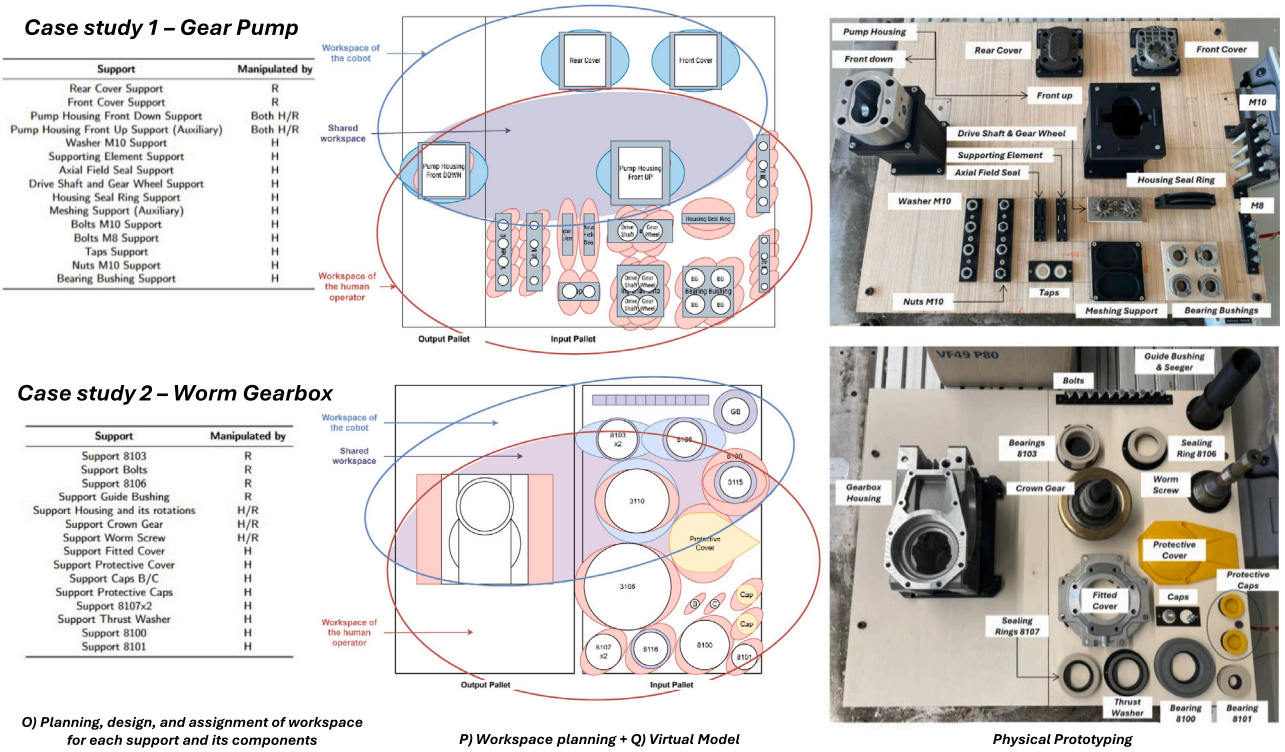

Fig. 10. Pallet design and physical prototyping with 3D printed supports for both case studies (gear pump at the top, worm gearbox at the bottom). Steps O and P belong to Phase 2, while Step Q is part of Phase 3.

Table 4
Impact parameters in the gear pump case: comparison between the original manual assembly and the virtual collaborative process.

	Impact parameters			
	Cycle time	Max LI index	Max RULA index	H's critical tasks
Original	5 min 17 s	1 (low)	3 (moderate)	4
Virtual model	4 min 40 s	1 (low)	1 (low)	0

As summarized in Table 4, the data shows a reduction in the number of critical or to-be-reduced tasks assigned to the human operator, from 4 to 0. Additionally, the maximum RULA score decreased from 3 (moderate risk) to 1 (low risk). Meanwhile, the NIOSH LI index remained unchanged at 1, indicating a low-risk level.

4.2. Case 2: Worm gearbox

The second case study focuses on a right-angle worm gearbox. As shown in the exploded view in Fig. 11, its key components are: (i) the input shaft, which includes the worm gear, and (ii) the output shaft, comprising the crown gear. These two shafts are positioned at a 90° angle to each other.

In line with the previous case study, the input data for Phase 1 consists of the assembly sequence provided by Bonfiglioli, the equipment (fixed setup), the ergonomic limits, and the product metrics. The gearbox under consideration has a total mass of 8.5 kg (though all its parts do not exceed 3 kg) and dimensions of 222.5 × 200 × 130.5 mm (bounding box: length, width, and height). In this case study, the initial requirements are ergonomic improvement and cycle time reduction compared to the original assembly process. These gearboxes are typically assembled on semi-automated production lines that alternate between human operators and press machines. In this work, the original process is adapted for fully manual assembly by replacing the hydraulic press with manual pressing performed by a single operator using appropriate tools.

4.2.1. Phase 1

From the task list of assembly manual, pallet refilling and component inspection have been excluded, assuming the components are pre-arranged on the pallet and pre-checked before entering the assembly workstation. Leakage tests, rotational tests, and oil filling have also been omitted, as they require specialized equipment and are typically conducted in later performance-check stages.

In **Step A**, the core assembly tasks are extracted and listed in Table 5. The required tools include lubrication tools, fastening tools, press-fitting tools, and a guide bushing for inserting the seeger ring. The assembly follows a structured sequence: first, assemble the output shaft and insert it into the housing, then complete the input shaft assembly and place it inside the housing. Finally, install the sealing elements to secure the final assembly. During **Step B**, the tasks are grouped as shown in Table 6. Given the numerous subassemblies in the gearbox, the original process with 40 tasks, many involving press-fitting a component onto another, has been reduced to 18 tasks. Each high-level press-fitting task now encompasses lubrication, grasping, releasing, and the press-fitting of the component. The constraints introduced address both the logical precedence between components and assembly-specific limitations. For example, bearing 8101 must be positioned (task 2) before inserting the crown gear into the housing (task 5), as there would be insufficient space to press-fit the bearing afterward.

The explicit definition of constraints identifies four sequences and four standalone tasks. The flowchart highlighting these dependencies, obtained in **Step C**, is shown in Fig. 12. The initial positions of the worm gear and housing are defined in **Step D**, as they undergo multiple rotations during assembly. In the manual, also the rotation of the crown gear is specified, although here can be omitted due to the symmetry of this component relative to the insertion plane. In **Step E**, the tasks are divided into subtasks. For the press-fitting tasks, which are the majority, lubrication was either included or omitted based on the original assembly process, in line with the assembly manual guidelines. The seeger ring insertion (task 8) was further detailed to incorporate the use of the guide bushing.

Number	Component
3100	Gearbox Housing
3105	Fitted Cover
3110	Crown Gear
3115	Worm Gear
3125	Input Protection Cover
8100	Bearing
8101	Bearing
8103	Bearing
8106	Sealing Ring
8107	Sealing Ring
8112	O-Ring
8115	Seeger
8116	Thrust Washer
8120	Fitted Cover Screws
8135A	Tap Oil Plug
8135B	Oil Plug (on housing)
8135C	Vent Plug
/	Output Protective Caps

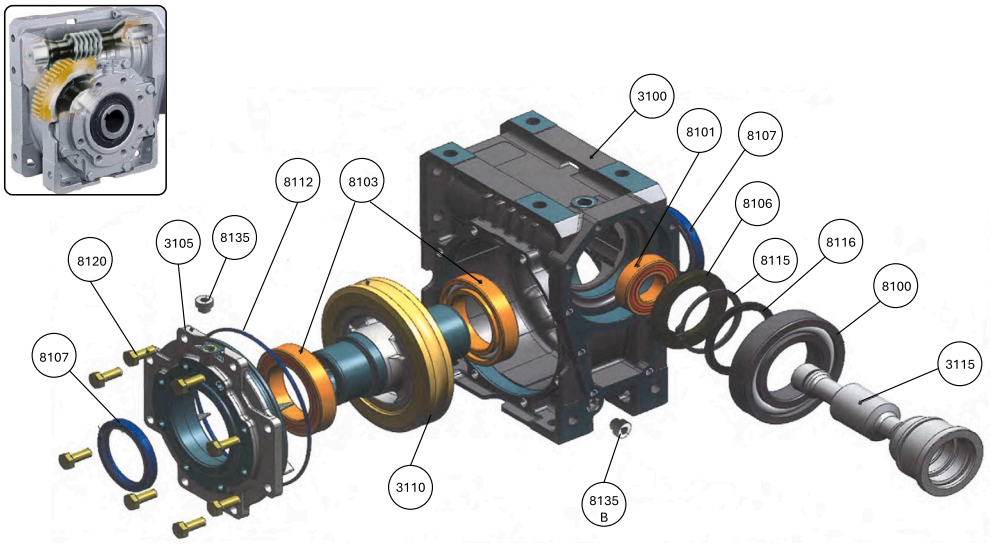

Fig. 11. 3D model of the worm gearbox and part list.

Table 5
Main task list extracted from the assembly manual of the worm gearbox. The list excludes component refilling and quality checks, leakage tests, rotational tests and oil filling.

Step	Description	Required tools	Additional notes
1	Lubricate the sealing ring seat 8106.	Lubrication	
2	Lubricate the inner seat of sealing ring 8106	Lubrication	
3	Pre-position sealing ring 8106 on the housing.		Worm gear side
4	Pre-position bearing 8101 in the housing.		Worm gear side
5	Place the worm gear on bearing 8100.		
6	Press-fit sealing ring 8106 onto the housing.	Press-fitting tool	
7	Press-fit bearing 8101 onto the housing.	Press-fitting tool	
8	Press-fit worm gear on bearing 8100.	Press-fitting tool	
9	Rotate the housing.		Worm gear side lateral
10	Lubricate the cover seat.	Lubrication	
11	Pre-position bearing 8103 on crown gear.		
12	Retrieve, rotate and insert crown gear with 8103 into the housing.		
13	Pre-position bearing 8103 on the crown gear.		
14	Rotate and place worm gear with 8100 on the lower support.		
15	Retrieve the guide bushing and insert it on the worm gear	Guide bushing	
16	Insert thrust washer on worm gear.		
17	Insert Seeger ring in the guide bushing.		
18	Press-fit bearing 8103 onto the housing.	Press-fitting tool	
19	Press-fit crown gear onto bearing 8103.	Press-fitting tool	
20	Press-fit bearing 8103 onto crown gear.	Press-fitting tool	
21	Press-fit Seeger ring onto worm gear.	Press-fitting tool	
22	Pre-position cover on the housing.		
23	Pre-position screws 8102 on the cover.		x8
24	Remove the guide bushing.		
25	Press-fit cover onto the housing.	Press-fitting tool	
26	Tighten screws 8102.	Screwing	x8
27	Lubricate sealing ring 8107.	Lubrication	
28	Pre-position sealing ring 8107 on the housing.		Cover side
29	Rotate the housing.		Worm gear side up
30	Lubricate sealing ring 8107.	Lubrication	
31	Pre-position sealing ring 8107 on the opposite side.		
32	Retrieve, rotate, and mesh worm gear with crown gear.		
33	Insert vent plug 8135C into STGL housing.		
34	Insert sealed plug 8135B into STGL housing.		
35	Press-fit worm gear into the housing.	Press-fitting tool	
36	Press-fit two sealing rings 8107 (keeping the housing vertical).	Press-fitting tool	
37	Tighten 8135 into the housing.	Screwing	
38	Apply protective caps to the crown gear.		x2
39	Apply protection cover.		Worm gear side
40	Tighten screws on the protection cover.	Screwing	x2

4.2.2. Phase 2

Within **Step F**, the subtask evaluation identified some critical issues in human lifting and reorientation of the housing, particularly in the final phase of the assembly, when it is additionally loaded with the crown gear and the worm gear. More specifically, the ergonomic analysis conducted with Process Simulate confirmed these concerns, considering such tasks with moderate risk (i.e. lifting and rotation of the housing, lifting of the crown gear), where RULA index is equal to 4 in both cases.

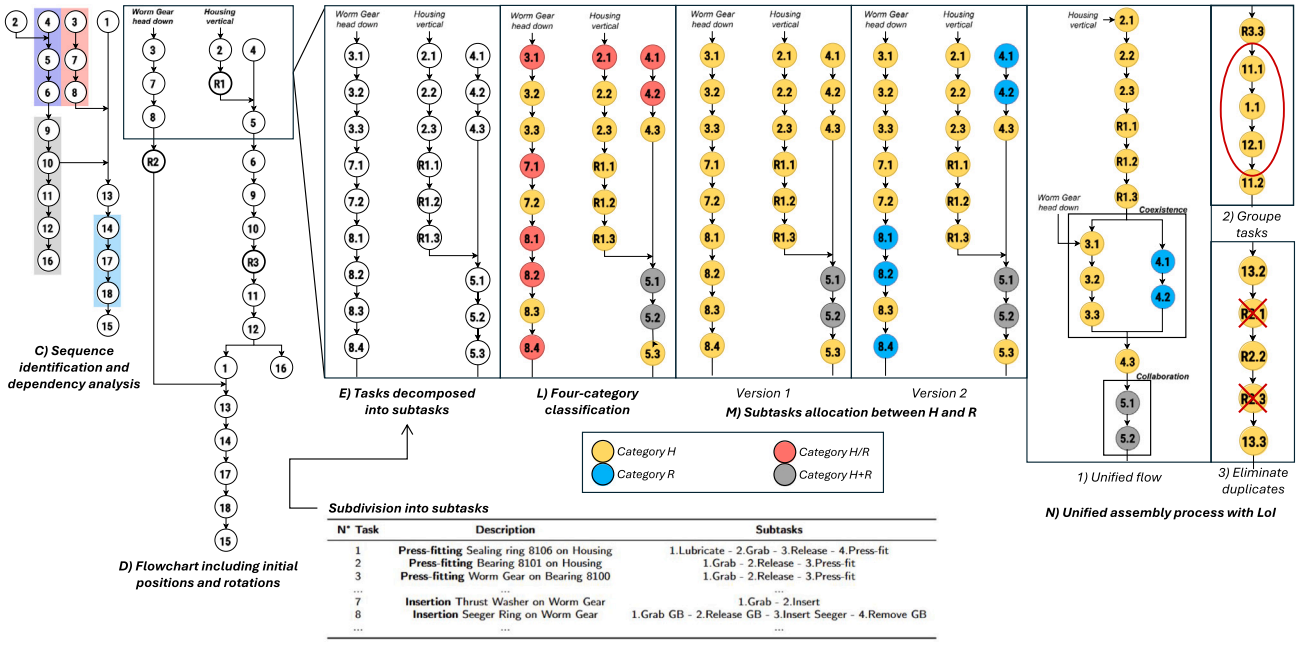

Fig. 12. Development of the collaborative assembly flow in the worm gearbox case. Steps C to E belong to Phase 1. Steps L to *N* are part of Phase 2, and are preceded by steps F to I (not shown in the image).

Table 6
List of higher-level tasks after Step B for the worm gearbox case.

Task	Description	Constraints
1	**Press-fitting** Sealing ring 8106 on housing	
2	**Press-fitting** Bearing 8101 on housing	
3	**Press-fitting** Worm gear on bearing 8100	
4	**Press-fitting** Bearing 8103 on housing	
5	**Press-fitting** Crown gear on housing	After 2,4
6	**Press-fitting** Bearing 8103 on crown gear	After 5
7	**Insertion** Thrust washer on worm gear	After 3
8	**Insertion** Seeger ring on worm gear	After 7
9	**Press-fitting** Cover on housing	After 6
10	**Screwing** The cover	After 9
11	**Press-fitting** Sealing ring 8107 on cover	After 10
12	**Press-fitting** Sealing ring 8107 on housing	After 11
13	**Meshing** Worm gear with crown gear in housing	After 1,2,8,10
14	**Positioning** Plug 8135C in STGL compartment	After 13
15	**Screwing** Plug 8135B in STGL compartment	After 18
16	**Insertion** Caps on crown gear	After 12
17	**Positioning** Protection cover on housing	After 14
18	**Screwing** The protection cover	After 17

After completing the evaluations in (**Step G-H-I**), in **Step L** all tasks resulted assigned to one of the four categories (H, R, H/R or H+R). As shown in Fig. 12, task 5 related to the manipulation of the crown gear is classified as a collaborative task (H+R), taking into consideration the possibility of exploiting the hand-guiding control mode, where the human operator actively guides the robot by physically interacting with the end-effector. This choice is due to the complexity of the insertion of the crown gear, which requires the human sensitivity to properly fit the components. However, with a component mass of 3 kg, the robot can validly assist the human operator by carrying the load, counteracting the gravity to reduce the physical strain. With this assignment, one of the previously identified critical tasks for the human is not assigned to category H.

During **Step M**, by analyzing each task individually, it becomes evident that almost none of them can be entirely performed by the robot. As a result, the first attempt allocation assigned nearly all tasks to the human, except for task 5, which is still collaborative. After reiterating the process with the aim to achieve a more balanced distribution, some tasks are split as visible in Fig. 12, where both diagrams are reported for comparison. For instance, most press-fitting tasks can be assigned to the robot, except for the press-fitting subtask and, if present, the lubrication subtask. This first refinement resulted in a more balanced distribution of tasks between H and R, allowing to proceed to the next step.

Based on the task allocation and the LoI introduced in Section 2.2.2, a unified process flow was developed, and each subtask was analyzed to identify possible parallelization. The grouping and sequential execution of multiple lubrication subtasks assigned to H were aimed at saving time by minimizing tool changes. Similarly, assigning consecutive tasks to H or R facilitates overlapping similar tasks. For instance, subtask 13.2 (grasping the worm gear) is identical to the first subtask of the rotation task (R2.1), so placing them consecutively eliminates the need for one of the two. The same applies to tasks R2.3 and 13.3, both involving component release. These considerations are presented in **Step N** of Fig. 12: image 1 illustrates the unified assembly flow, image 2 shows the grouping of lubrication (subtasks 1.1, 11.1, 12.1), whereas image 3 highlights the elimination of duplicate subtasks.

Considering the newly created single-flow process and with reference to the approach proposed in Fig. 5, **Step O** focuses on designing and drafting the supports. Each support begins with the analysis of its associated component. For example, the support containing the housing will be used to manage all its rotations. In **Step P**, after determining the footprint of each component and support, the input and output pallets are defined. As in the previous case of the pump (see Section 4.1.2) and following the methodology guidelines (see Section 2.2.3), the following points are applied: (i) the relative position of the human operator and the robot is fixed to 1 m as in the previous case, (ii) depending on which actor manipulates the component, its corresponding support is placed in either the shared or non-shared workspace, (iii) components are positioned to the right of the operator for easier gripping, with the output pallet on the left, (iv) higher components and supports (e.g., the

guide bushing and worm gear) are placed as far as possible, always on the right, (v) a more conservative manipulation area is assigned for reorienting the housing, as it is handled by both actors and its lifting and rotation space is unpredictable, (vi) the crown gear is positioned horizontally in relation to its insertion point in the housing, as is done with the worm gear, and (vii) while space optimization is not a critical factor, components are placed as close as possible, utilizing space as an additional degree of freedom.

4.2.3. Phase 3

The virtual model developed for the case 1 in Section 4.1.3 have been modified in **Step Q** to incorporate the new geometries (i.e. worm reducer parts and pallets). Then, during **Step R**, the new targets and paths are defined. A new robot code has been generated to implement the designed sequencing, adopting the same structure (procedures and commands) of the previous case study. However, in this case, a novel procedure has been developed for task 5. In particular, the procedure starts with the enabling signal from the manual button (pressed by the operator) and activates the hand-guiding mode. It must be underlined that in the simulation this task has been assigned to the robot for simplicity, with the human following the movements. Despite this, the mentioned procedure is established for the subsequent physical prototyping.

Finally, in **Step S**, the performance of the newly created process was evaluated. The following conclusions can be drawn:

1. The ergonomic requirements were partially met: the number of housing reorientation was reduced from three (original assembly) to two (collaborative assembly) and the crown gear lifting was made collaborative for weight compensation using hand-guiding mode, eliminating its rotation task. Additionally, the NIOSH analysis conducted using Process Simulate provided a LI value ranging between 1 and 3 (moderate risk level) for the remaining rotation tasks.
2. The adjustment made in **Step M** enhanced parallelization, achieving an acceptable cycle time. Without this modification, the designer would have been redirected to **Step N**, revealing the imbalance between tasks assigned to R and H. This would have triggered an iterative cycle leading back to **Step M** and resulting in a second version of the virtual model.
3. The input data does not provide specific information on the cycle time for assembling a single gearbox, as it is part of a semi-automated line. Therefore, as a starting point, the time obtained by applying the Boothroyd & Dewhurst method is considered, resulting in 6 min and 30 s. However, the time allocated for pressing components was underestimated (3.5 s), while practical tests showed a duration of at least 7 s. Thus, for a more precise reference, the fully manual process has been replicated (see Section 4.3), yielding an average assembly time of 7 min and 39 s. With a cycle time of 6 min and 55 s in the simulated collaborative process, the requirement is met (reduction of 9.6% compared to the original process).

Table 7 summarizes the data using the same approach as the previous case study. While the maximum ergonomic risk levels, as indicated by the RULA and NIOSH LI indices, remain unchanged, the number of critical or to-be-reduced tasks assigned to the human operator has decreased from 5 to 2, confirming an overall improvement in the operator's working conditions. The unchanged index values are attributed to the fact that certain tasks, although categorized as to-be-reduced, could not be reassigned to the robot and thus remained with the human operator.

Table 7
Impact parameters in the worm gearbox case: comparison between the original manual assembly and the virtual collaborative process.

	Impact parameters			
	Cycle time	Max LI index	Max RULA index	H's critical tasks
Original	7 min 39 s	2 (moderate)	4 (moderate)	5
Virtual model	6 min 55 s	2 (moderate)	4 (moderate)	2

4.3. Validation tests on physical cell

The aim of this section is to validate the proposed framework by testing the operability of the designed collaborative cells, based on the two collaborative processes developed in Sections 4.1 and 4.2, assessing the resulting cycle time, and verifying the absence of critical issues in the execution of tasks performed by both the human operator and the robot. The assembly processes were tested on the physical cell described in Section 3. Specifically, the robot code was generated for both case studies and downloaded to the OmniCore C30 controller. In both scenarios, 3D-printed supports were used to prepare the pallets, as illustrated in Fig. 10. The assembly process was repeated 20 times to account for the natural variability introduced by the human operator, which is less repeatable compared to the virtual counterpart. The obtained results are reported in Fig. 13, where a comparison between the original and collaborative assemblies is provided over the 20 trials.

For the pump assembly, the average cycle time was 4 min and 37 s, representing a 12.6% reduction compared to the original process time of 5 min and 17 s. This result is close to the 4 min and 40 s achieved in the simulation. The slight reduction is attributed to the variability of human behavior, as occasional faster actions are difficult to model in the virtual environment. For the gearbox assembly, an average time of 7 min and 3 s was recorded, showing a 7.8% reduction compared to the original 7 min and 39 s. This was slightly longer than the 6 min and 55 s obtained in the simulation. The difference is again attributed to the inherent challenge of accurately modeling the human behavior, particularly in tasks like meshing the worm gear and the crown gear.

The physical tests confirmed the validity of the design method, as demonstrated by the close alignment between the obtained process times and those predicted by the simulations. Overall, the initial requirements are met, with the resulting processes exhibiting adequate task balancing and ensuring that both the operator and the robot work under feasible conditions with effective task parallelization. Fig. 14 illustrates four frames from the gearbox assembly process, highlighting tasks performed with different LoI, namely task 8.2 and 8.3 (synchronization), 9 and 8.4 (coexistence), 10 (cooperation) and 5 (collaboration). In the first frame, the different timing between robot and operator tasks can be deduced from the green light, indicating that the robot is in standstill mode (ready for operation). Conversely, in the remaining frames the robot is busy. The last frame shows the hand-guiding mode active in the case of collaboration (assisted positioning of the crown gear in the housing).

The complete research dataset, including all files generated from **Step A** to **Step S** and corresponding process videos, is provided in the supplementary material.

5. Conclusions

This work proposes and validates a structured framework for the integrated design of human–robot collaborative assembly workstations, aimed at optimizing task allocation considering both ergonomic safety and process efficiency. The methodology is organized into three iterative phases, starting with the analysis of the assembly process, followed by task classification and allocation between humans and robots, and concluding with virtual prototyping, simulation, and performance optimization of the collaborative cell. The aim is to provide a practical,

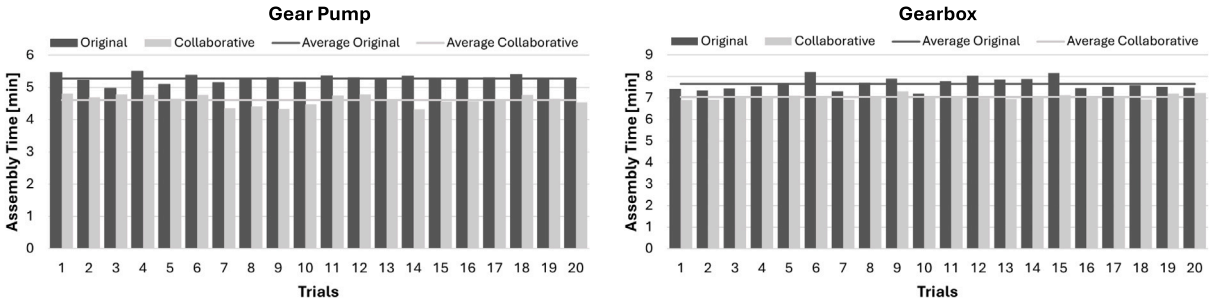

Fig. 13. Assembly times obtained during physical validation: original vs. collaborative processes.

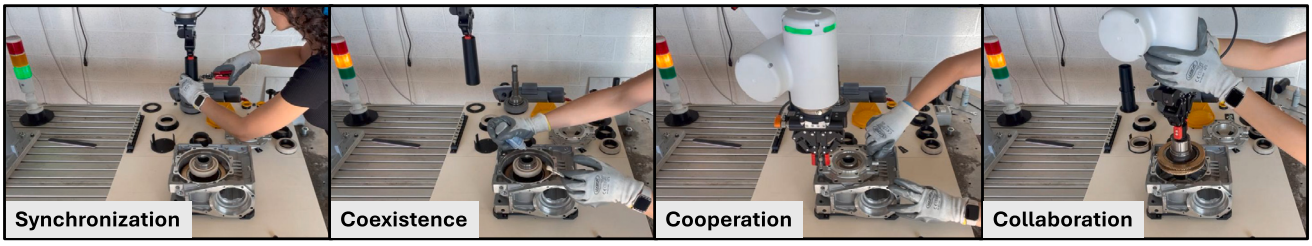

Fig. 14. Frames extracted from the gearbox assembly process with different LoI: collaboration (hand-guiding mode), synchronization, coexistence and cooperation.

accessible, and scalable approach for transitioning traditional manual assembly processes into collaborative ones, supporting the Industry 5.0 vision of human-centric automation. In the second part of the paper, the framework has been validated through two industrial case studies with different product and process characteristics and constraints: a gear pump and a worm gearbox. The validation highlighted that one of the main challenges in designing collaborative cells through iterative approaches, such as the proposed framework, lies in managing the complexity of design revisions. The framework addresses this issue by explicitly guiding the designer back to the appropriate step whenever specific requirements are not met. The validation process also provided clear examples of such decision points, demonstrating the framework's effectiveness in supporting the designer, while offering valuable insights into the critical questions that must be addressed during cell design. For validation purpose, after completing the design phases, both assembly processes were tested on a physical collaborative cell at the university laboratory. In particular, the supports for parts were prototyped with a 3D printer and the robot code produced during simulation was imported into the real robot controller with few adjustments, enabling the replication of the full processes. The experimental results demonstrated a close alignment between the cycle times predicted during simulation in Process Simulate and the ones achieved during experimentation, confirming the validity of the proposed methodology. The framework also showcased effective task balancing, ergonomic risk mitigation, and task parallelization with different LoI between human operators and cobots. Overall, the proposed framework remains effective regardless of the specific simulation tools or equipment adopted, ensuring its suitability across diverse industrial contexts.

Future work will aim to expand the framework beyond the design phase, integrating cognitive workload assessment (e.g., NASA-TLX) and user experience analysis tools (e.g., camera tracking, voice feedback). Extensions may also include cost–benefit analysis and support for multi-operator scenarios. These additions will support its application in real-time production environments, enabling monitoring, operator assistance, and dynamic task reallocation.

CRediT authorship contribution statement

Martina Salami: Conceptualization, Data curation, Investigation, Software, Validation, Writing – original draft. **Pietro Bilancia:** Conceptualization, Formal analysis, Supervision, Writing – original draft, Methodology. **Margherita Peruzzini:** Conceptualization, Methodology, Writing – review & editing. **Marcello Pellicciari:** Conceptualization, Funding acquisition, Project administration, Writing – review & editing.

Funding sources

This research was funded by the European Community's Horizon Europe programme under grant agreement No. 101091780 (DaCapo).

Declaration of competing interest

The authors declare that they have no known competing financial interests or personal relationships that could have appeared to influence the work reported in this paper.

Supplementary material

The research data related to this work can be freely downloaded at this repository link.

Data availability

Data will be made available on request.

References

[1] A. Weiss, A.-K. Wortmeier, B. Kubicek, Cobots in industry 4.0: A roadmap for future practice studies on human–robot collaboration, IEEE Trans. Hum. Mach. Syst. 51 (4) (2021) 335–345.

[2] M.R. Pedersen, L. Nalpantidis, R.S. Andersen, C. Schou, S. Bøgh, V. Krüger, O. Madsen, Robot skills for manufacturing: From concept to industrial deployment, Robot. Comput.-Integr. Manuf. 37 (2016) 282–291.

[3] A. Weiss, R. Buchner, M. Tscheligi, H. Fischer, Exploring human-robot cooperation possibilities for semiconductor manufacturing, in: 2011 International Conference on Collaboration Technologies and Systems, CTS, IEEE, 2011, pp. 173–177.

[4] P.M. Fitts, Human engineering for an effective air-navigation and traffic-control system., Ohio State Univ. Res. Found. Columb. (1951).

[5] S. Nahavandi, Industry 5.0—A human-centric solution, Sustain. 11 (16) (2019) 4371.

[6] M. Peruzzini, E. Prati, M. Pellicciari, A framework to design smart manufacturing systems for industry 5.0 based on the human-automation symbiosis, Int. J. Comput. Integr. Manuf. 37 (10–11) (2024) 1426–1443.
[7] E. Prati, V. Villani, F. Grandi, M. Peruzzini, L. Sabattini, Use of interaction design methodologies for human–robot collaboration in industrial scenarios, IEEE Trans. Autom. Sci. Eng. 19 (4) (2021) 3126–3138.
[8] A. Kolbeinsson, E. Lagerstedt, J. Lindblom, Foundation for a classification of collaboration levels for human-robot cooperation in manufacturing, Prod. Manuf. Res. 7 (1) (2019) 448–471.
[9] S. Hopko, J. Wang, R. Mehta, Human factors considerations and metrics in shared space human-robot collaboration: A systematic review, Front. Robot. 9 (2022) 799522.
[10] J. Saenz, R. Behrens, E. Schulenburg, H. Petersen, O. Gibaru, P. Neto, N. Elkmann, Methods for considering safety in design of robotics applications featuring human-robot collaboration, Int. J. Adv. Manuf. Technol. 107 (2020) 2313–2331.
[11] N. Pedrocchi, F. Vicentini, M. Matteo, L.M. Tosatti, Safe human-robot cooperation in an industrial environment, Int. J. Adv. Robot. Syst. 10 (1) (2013) 27.
[12] P. Bilancia, J. Schmidt, R. Raffaeli, M. Peruzzini, M. Pellicciari, An overview of industrial robots control and programming approaches, Appl. Sci. 13 (4) (2023) 2582.
[13] M. Lorenzini, M. Lagomarsino, L. Fortini, S. Gholami, A. Ajoudani, Ergonomic human-robot collaboration in industry: A review, Front. Robot. 9 (2023) 813907.
[14] Š. Václav, P. Pokorný, A. Kamenszká, A part as an object of assembly, World J. Eng. Technol. 9 (4) (2021) 904–915.
[15] I. Palomba, L. Gualtieri, R. Rojas, E. Rauch, R. Vidoni, A. Ghedin, Mechatronic re-design of a manual assembly workstation into a collaborative one for wire harness assemblies, Robotics 10 (1) (2021) 43.
[16] J. Krüger, T.K. Lien, A. Verl, Cooperation of human and machines in assembly lines, CIRP Ann 58 (2) (2009) 628–646.
[17] L. Duarte, M. Neves, P. Neto, Benchmarking human-robot collaborative assembly tasks, Results Eng. 22 (2024) 102042.
[18] J. Saenz, N. Elkmann, O. Gibaru, P. Neto, Survey of methods for design of collaborative robotics applications-why safety is a barrier to more widespread robotics uptake, in: Proceedings of the 2018 4th International Conference on Mechatronics and Robotics Engineering, 2018, pp. 95–101.
[19] L. Gualtieri, E. Rauch, R. Vidoni, D.T. Matt, An evaluation methodology for the conversion of manual assembly systems into human-robot collaborative workcells, Procedia Manuf. 38 (2019) 358–366.
[20] J.C. Mateus, D. Claeys, V. Limère, J. Cottyn, E.-H. Aghezzaf, A structured methodology for the design of a human-robot collaborative assembly workplace, Int. J. Adv. Manuf. Technol. 102 (2019) 2663–2681.
[21] M. Dalle Mura, G. Dini, Designing assembly lines with humans and collaborative robots: A genetic approach, CIRP Ann 68 (1) (2019) 1–4.
[22] A.C. Simões, A. Pinto, J. Santos, S. Pinheiro, D. Romero, Designing human-robot collaboration (HRC) workspaces in industrial settings: A systematic literature review, J. Manuf. Syst. 62 (2022) 28–43.
[23] S.K. Andersson, A. Granlund, M. Hedelind, J. Bruch, Exploring the capabilities of industrial collaborative robot applications, in: SPS2020, IOS Press, 2020, pp. 109–118.
[24] T.R. Waters, V. Putz-Anderson, A. Garg, L.J. Fine, Revised NIOSH equation for the design and evaluation of manual lifting tasks, Ergon. 36 (7) (1993) 749–776.
[25] F. Ranz, V. Hummel, W. Sihn, Capability-based task allocation in human-robot collaboration, Procedia Manuf. 9 (2017) 182–189.
[26] A.A. Malik, A. Bilberg, Complexity-based task allocation in human-robot collaborative assembly, Ind. Robot. Int. J. Robot. Res. Appl. 46 (4) (2019) 471–480.
[27] L. Gualtieri, I. Palomba, F.A. Merati, E. Rauch, R. Vidoni, Design of human-centered collaborative assembly workstations for the improvement of operators' physical ergonomics and production efficiency: A case study, Sustain. 12 (9) (2020) 3606.
[28] M. Gómez-Galán, J. Pérez-Alonso, Á.-J. Callejón-Ferre, J. López-Martínez, Musculoskeletal disorders: OWAS review, Ind. Health 55 (4) (2017) 314–337.
[29] O. Karhu, R. Härkönen, P. Sorvali, P. Vepsäläinen, Observing working postures in industry: Examples of OWAS application, Appl. Ergon. 12 (1) (1981) 13–17.
[30] N. Fığlalı, A. Cihan, H. Esen, A. Fığlalı, D. Çeşmeci, M.K. Güllü, M.K. Yılmaz, Image processing-aided working posture analysis: I-OWAS, Comput. Ind. Eng. 85 (2015) 384–394.
[31] E. Corlett, H.W. Discomfort, Rapid upper limb assessment (RULA), Occup. Ergon. Handb. (1998) 437.
[32] L. McAtamney, E.N. Corlett, RULA: a survey method for the investigation of work-related upper limb disorders, Appl. Ergon. 24 (2) (1993) 91–99.
[33] C.E.f.M.M. Stephen Bowden, Rapid upper limb assessment (RULA) worksheet tool – A step by step guide [online], 2024.
[34] T.R. Waters, M.-L. Lu, L.A. Piacitelli, D. Werren, J.A. Deddens, Efficacy of the revised NIOSH lifting equation to predict risk of low back pain due to manual lifting: expanded cross-sectional analysis, J. Occup. Environ. Med. 53 (9) (2011) 1061–1067.
[35] V.M. Ciriello, S.H. Snook, L. Hashemi, J. Cotnam, Distributions of manual materials handling task parameters, Int. J. Ind. Ergon. 24 (4) (1999) 379–388.
[36] D. Kee, Systematic comparison of OWAS, RULA, and REBA based on a literature review, Int. J. Environ. Res. Public Heal. 19 (1) (2022) 595.
[37] D. Colombini, Risk Assessment and Management of Repetitive Movements and Exertions of Upper Limbs: Job Analysis, Ocra Risk Indicies, Prevention Strategies and Design Principles, Elsevier, 2002.
[38] M. Faccio, I. Granata, R. Minto, Task allocation model for human-robot collaboration with variable cobot speed, J. Intell. Manuf. 35 (2) (2024) 793–806.
[39] F. Chen, K. Sekiyama, F. Cannella, T. Fukuda, Optimal subtask allocation for human and robot collaboration within hybrid assembly system, IEEE Trans. Autom. Sci. Eng. 11 (4) (2013) 1065–1075.
[40] O. Salunkhe, J. Stahre, D. Romero, D. Li, B. Johansson, Specifying task allocation in automotive wire harness assembly stations for human-robot collaboration, Comput. Ind. Eng. 184 (2023) 109572.
[41] G. Boschetti, M. Faccio, I. Granata, Human-centered design for productivity and safety in collaborative robots cells: A new methodological approach, Electron. 12 (1) (2022) 167.
[42] E. Merlo, E. Lamon, F. Fusaro, M. Lorenzini, A. Carfi, F. Mastrogiovanni, A. Ajoudani, Dynamic human-robot role allocation based on human ergonomics risk prediction and robot actions adaptation, in: 2022 International Conference on Robotics and Automation, ICRA, IEEE, 2022, pp. 2825–2831.
[43] G. Michalos, J. Spiliotopoulos, S. Makris, G. Chryssolouris, A method for planning human robot shared tasks, CIRP J. Manuf. Sci. Technol. 22 (2018) 76–90.
[44] D. Antonelli, G. Bruno, et al., Dynamic task sharing strategy for adaptive human-robot collaborative workcell, DEStech Trans. Eng. Technol. Res.(Icpr) (2017).
[45] L.S. Scimmi, M. Melchiorre, M. Troise, S. Mauro, S. Pastorelli, A practical and effective layout for a safe human-robot collaborative assembly task, Appl. Sci. 11 (4) (2021) 1763.
[46] P. Segura, O. Lobato-Calleros, I. Soria-Arguello, E.G. Hernández-Martínez, Work roles in human–robot collaborative systems: Effects on cognitive ergonomics for the manufacturing industry, Appl. Sci. 15 (2) (2025) 744.
[47] P. Neto, M. Simão, N. Mendes, M. Safeea, Gesture-based human-robot interaction for human assistance in manufacturing, Int. J. Adv. Manuf. Technol. 101 (2019) 119–135.
[48] S. Secil, M. Ozkan, Minimum distance calculation using skeletal tracking for safe human-robot interaction, Robot. Comput.-Integr. Manuf. 73 (2022) 102253.
[49] ABB, GoFa CRB 15000, 2025, URL https://new.abb.com/products/robotics/robots/collaborative-robots/crb-15000. (Accessed October 2024).
[50] I. Bettles, Design for manufacture & assembly (DFMA)-the boothroyd & dewhurst approach, in: 1992 Third International Conference on Factory 2000, 'Competitive Performance Through Advanced Technology', 1992, pp. 316–321.